PNAS
www.pnas.org

Supplementary Information for

Cholinergic suppression of hippocampal sharp wave ripples impairs working memory

Yiyao Zhang[1,a], Liang Cao[1,5,a], Viktor Varga[1], Miao Jing[6,7], Mursel Karadas[1], Yulong Li[6] and
György Buzsáki[1,2,3,4,*]

Corresponding authors: György Buzsáki
Email: gyorgy.buzsaki@nyumc.org

This PDF file includes:

SI Materials and Methods

Surgical Procedure. All experiments were approved by the Institutional Animal Care and Use Committee at New York University Langone Medical Center (NYULMC). General anesthesia was induced with isoflurane inhalation. For survival surgery (injection of virus, or implantation of thermometer and optical fibers), anesthesia was maintained by isoflurane through a mask mounted on the stereotaxic apparatus. Body temperature was kept constant with a heating pad (37 ℃).

Virus injection. The skull was exposed under antiseptic conditions using local anesthesia with bupivacaine/lidocaine, and holes were drilled above hippocampus CA1 [Hippocampus: AP – 2.3 mm, ML ±2.00 mm]. A glass pipette (30- to 50-μm tip) connected to a Nanoject II/Nanoliter 2000 microinjector (Drummond Scientific Co. or WPI Inc.) was used to inject 0.1 μL of ACh3.0-mutant virus [1] solution at 1.5 mm depths of Hippocampal CA1, over 15 min. After injection the pipette was removed slowly (0.1 then 0.5-mm steps, 10-min waiting periods between each) and the scalp was sutured.

Thermometer and optical fiber implantation. In the MS, a 105-μm-diameter optical fiber was implanted at depth 3.2 mm with thermometer. Before surgery, the optic fiber was stripped from the outer layer and connection with 1.25-mm ceramic ferrules (extracted from LC connectors; Thorlabs). A pencil-shaped tip was obtained by etching for 30 s in hydrofluoric acid (Sigma) to facilitate the insertion in the brain and increase light scattering.

Mutant ACh3.0 fluorescent signal. A 400 μm diameter optic fiber was implanted above the pyramidal cell layer to collect the fluorescent signal from CA1 area. During recording, 400 Hz square wave, driven LED (473nm) was used to excite ACh3.0-mutant sensor. The raw ACh3.0 fluorescent signal recorded by fiber photometry which was filtered through a 20Hz lowpass hardware filter and then stored for subsequent analysis. All equipment is same as the experiment of ACh3.0 signal. The ACh3.0-mutant fluorescent response was obtained using the equation $\Delta F/F = (F - F_0)/F_0$, in which the F_0 is the baseline signal detected by a 5^{th} order polynomial fitting.

Behavioral speed. Position was tracked with the OptiTrack camera system. IR reflective markers were mounted in unique positions on each animals' head stage and imaged simultaneously by six cameras (Flex 3) placed above the behavioral apparatus. Calibration across cameras allowed for the three-dimensional reconstruction of the animals' head position, and head orientation, to within 1 mm (avg. displacement error = 0.70 mm ± 1.5 mm) at 100 Hz. Position data were analyzed and segmented using a custom MATLAB software suite.

Temperature measurement.

Modeling in C. We simulated the light distribution using the Monte Carlo method, where the random walk of photon packets is traced through the tissue in 3 dimensions [2, 3]. We used optical parameters are given in [4]. For a given excitation wavelength, the scattering μ_s, absorption μ_a, and anisotropy g coefficients are determined as 10 mm^{-1}, 0.066 mm^{-1} and 0.9, respectively. Numerical calculation is carried out as in [5].

Light absorption by tissue generates heat. The amount of absorbed energy is defined by the source term, which is the product of the light irradiance (mW/mm^2) and the absorption coefficient a. Here, we describe the resulting temperature increase by the Pennes bioheat equation [6], which we simply by ignoring the convection term due to blood/fluid perfusion gives:

$$\rho C \frac{\partial T}{\partial t} = \nabla(k \nabla T) + \phi \mu_a$$

Constant ρ denotes the mass density (ρ = 1.04 x 10^3 kg/m^3), c the specific heat conductivity (C = 3.6 J/g-K) and k the thermal conductivity (k = 0.56 W/m-K) of the brain tissue. The forward finite difference method is used to solve the heat equation using a spatial step width of Δx = 0.01 mm, and ensuring numerical stability by adjusting the temporal step as given in

$$\Delta t \leq \frac{(\Delta x)^2}{6k} \rho C$$

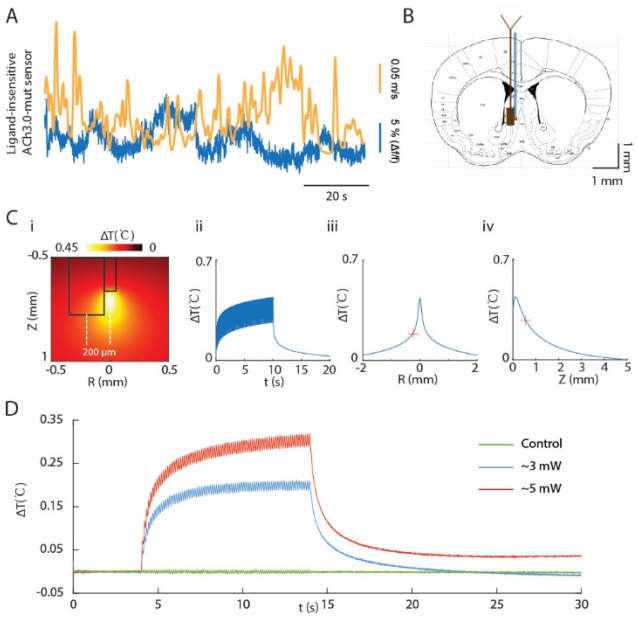

Supplemental Fig 1. ACh3.0-mut sensor's fluorescence signal is independent of animal's behavioral states, and temperature increasing by optogenetic stimulation

A. ACh3.0-mutant sensor was injected in hippocampal CA1. In this sham animal the fluorescence signal (blue) does not show behavior-dependence (yellow line, speed of locomotion).

B. Schematic diagram of temperature measurement in medial septum. Blue: optical fiber, brown: thermometer.

C. Heating model of optogenetic stimulation. Z: vertical distance from optical fiber tip. R: horizontal distance from optical fiber tip. Red dashed cross marker graphs ii, iii and iv: thermometer center.

D. Temperature measurement in medial septum in vivo with two different light intensities. n = 30 trials. Note temperature change < 0. 35 °C at the stronger (~5 mW) light intensity).

SI References

1. Jing, M., Li, Y., Zeng, J. et al. An optimized acetylcholine sensor for monitoring in vivo cholinergic activity. Nat Methods 17, 1139–1146 (2020).
2. L Wang, SL Jacques, L Zheng, Mcml—monte carlo modeling of light transport in multi-layered tissues. Comput. methods programs biomedicine 47, 131–146 (1995).
3. JM Stujenske, T Spellman, JA Gordon, Modeling the spatiotemporal dynamics of light and heat propagation for in vivo optogenetics. Cell reports 12, 525–534 (2015).
4. A Yaroslavsky, et al., Optical properties of selected native and coagulated human brain tissues in vitro in the visible and near infrared spectral range. Phys. Medicine & Biol. 47, 2059 (2002).
5. M. Karadas, "Highly Sensitive Magnetic Sensing of Neural Activity". Technical University of Denmark,Lyngby, Denmark (2019).

6. HH Pennes, Analysis of tissue and arterial blood temperatures in the resting human forearm. J. applied physiology 1, 29 93–122 (1948).